

# A *Hox* gene mutation that triggers nonsense-mediated RNA decay and affects alternative splicing during *Drosophila* development

Claudio R. Alonso\* and Michael Akam

Laboratory for Development and Evolution, Department of Zoology, University of Cambridge, Downing Street, Cambridge CB2 3EJ, UK

Received April 29, 2003; Accepted May 7, 2003

## ABSTRACT

**Nonsense mutations are usually assumed to affect protein function by generating truncated protein products. Nonetheless, it is now clear that these mutations affect not just protein synthesis but also messenger RNA stability. The surveillance mechanism responsible for the detection and degradation of ‘nonsense’ RNA messages is termed nonsense-mediated RNA decay (NMD). Essential biochemical components of the NMD machinery have been defined in several species. Here we identify the *Drosophila* orthologue of one of these factors, Upf1, and document its expression during embryogenesis. To test whether NMD acts during *Drosophila* development, we make use of a mutation that introduces a stop codon into a variably spliced exon of the *Hox* gene *Ultrabithorax* (*Ubx*). Using real-time quantitative RT-PCR we demonstrate that *Ubx* transcripts containing the premature stop codon are expressed at lower levels than their wild type counterpart. Unexpectedly, we also find that the same mutation significantly increases the levels of a *Ubx* splicing isoform that lacks the exon containing the premature termination codon. These findings indicate that NMD is operational during *Drosophila* development and suggest that nonsense mutations may affect development by altering the spectrum of splicing products formed, as well as by reducing or eliminating protein synthesis.**

## INTRODUCTION

Eukaryotes as diverse as yeast and humans use a common biochemical pathway to detect and degrade RNA messages that contain premature termination codons (PTCs) (1). Although the mechanistic details underlying this type of RNA surveillance are not entirely understood, information from the animal systems analysed so far, indicates that the triggering of effective nonsense-mediated RNA decay (NMD) demands two signals to be present in the mRNA: a termination codon, and the presence of an intron downstream of this

termination codon (1). Consistent with these requirements, mammalian intron-less genes are immune to NMD (2). Recent work performed in mammalian systems indicates that the second signal is probably not the intron itself but a ‘molecular label’ left after the intron is removed (3,4). This molecular label, the exon junction complex (EJC), has also been shown to be involved in the regulation of RNA export out of the nucleus (5,6). The binding of the EJC at a specific position on a given RNA message appears to be a key element for the distinction of PTCs from ordinary stop codons, which are mostly located in the final exon of the message (1,7,8). Additional support for this view is provided by experiments showing that artificial tethering of some members of the EJC, downstream of a regular termination codon, is sufficient to trigger NMD (9,10).

Since NMD also occurs in yeast, where only a small fraction of genes possesses introns, a somehow different mechanism must operate to identify PTC-bearing messages in this organism. Indeed, downstream sequence elements composed of degenerate AU-rich motifs have been shown to be essential *cis*-acting elements for the recognition of nonsense messages (11). In spite of these differences, in yeast as well as in humans, three interacting proteins, Upf1, Upf2 and Upf3, are necessary for effective NMD. Of these, Upf1 has been the one studied in most detail. The Upf1 protein is a member of the group I RNA helicases and has been shown to interact with the translation release factors eRF1 and eRF3, well in line with its role in NMD and translation termination (12). Tethering of Upf1 downstream of a termination codon was shown to be sufficient to trigger NMD (13).

In spite of the growing interest to explain the molecular mechanisms underlying NMD, fundamental aspects of this process remain mysterious. One unresolved issue is the question of where, within the cell, nonsense transcripts are destroyed. Mainstream opinion sustains the view that RNA degradation must occur somewhere in the cytoplasm (14). However, a growing number of examples suggests that nonsense messages can be recognised and degraded within the nucleus after detection by a mechanism of intra-nuclear scanning (15,16). Recent reports describing the existence of translation in the nucleus provide further support for these models (17,18).

Nonsense mutations have also been shown to affect pre-mRNA processing events, such as RNA splicing. This

\*To whom correspondence should be addressed. Tel: +44 1223 331773; Fax: +44 1223 336679; Email: cra21@hermes.cam.ac.uk

response, termed nonsense-associated altered splicing (NAS) consists of the increase of the levels of alternatively spliced transcripts that omit exons carrying nonsense codons (16,19). Two different types of NAS exist. One of them is triggered by nonsense mutations that disrupt splicing regulatory elements, which modulate the performance of alternative splicing reactions. The other type of NAS is based on an unidentified mechanism able to detect disruptions of the reading frame. Two recent articles provide strong evidence that, although both, NMD and frame-dependent NAS require the existence of a nonsense mutation and a translation-like process (20,21), they are functionally distinct processes that rely on different, but overlapping sets of proteins (22,23) [reviewed in (24)].

Another unresolved matter is the role of NMD (and NAS) in the normal biology of different organisms. In yeast for example, *Upf1* null mutants are viable showing only minor metabolic problems (25). In nematodes, elimination of the NMD pathway results in viable animals with slight morphological defects (26). In contrast, targeted disruption of the mouse gene *Rent1*, the murine orthologue of *Upf1*, is embryonic lethal, indicating that some functions of *Upf1* must be essential for some aspects of mouse development (27). Surprisingly, beyond this point there is no other information on the role played by the NMD pathway in animal development. This fact prompted us to investigate whether NMD was active during the embryonic development of the fruit fly *Drosophila melanogaster*.

For this purpose, we first searched the *Drosophila* genome for conserved genes encoding components of the NMD biochemical machinery. Our search identified the *Dm-Upf1* gene, which we show is dynamically expressed during embryogenesis. Secondly, we tested the activity of the NMD pathway by making use of a nonsense mutation that affects the *Hox* gene *Ultrabithorax* (*Ubx*) (28). *Drosophila Ubx* encodes a homeodomain transcription factor that regulates development in a particular region of the animal body (29). In normal development, the *Ubx* gene produces a family of protein isoforms through alternative splicing. Quantification of the abundance of two *Ubx* isoforms in wild type and *Ubx* nonsense-mutant embryos shows that: (i) messages containing the nonsense codon are expressed at lower levels than their wild type counterparts and (ii) in mutant embryos, mRNAs coding for a *Ubx* isoform that lacks the nonsense codon are present at higher levels than expected. These observations suggest that NMD is operational during *Drosophila* embryonic development and that nonsense mutations could potentially influence development by altering the ratio among splicing isoforms of the affected genes.

## MATERIALS AND METHODS

### Sequence alignment and phylogenetic analysis

A sequence similarity search of *Drosophila* data sets (Fly BLAST) using the human *Upf1* gene (HUPF1) as probe, identified the *Drosophila* gene *CG1559* and its protein product (SWISS PROT accession code Q9VYS3). Sequences were aligned using ESPript and loaded up in the TREE-puzzle program.

### Fly stocks and embryo collections

Stocks carrying the *Ubx*<sup>195</sup> allele were a kind gift from Javier Lopez. *Ubx* mutant chromosomes were balanced over TM6B balancer chromosomes carrying P{w<sup>+</sup>mW.hs:Ubi-GFP.S65T}PAD2 as provided from the Bloomington stock centre (<http://fly.bio.indiana.edu>). Populations of Oregon Red and *Ubx*<sup>195</sup> adult flies (age 7–14 days) were transferred to cages where embryos were collected on apple juice plates for ~1 h and then allowed to develop at 25°C for variable times.

### RNA *in situ* hybridisations and other procedures with embryo and larvae

An exonic fragment of *DmUpf1* was amplified from Oregon Red genomic DNA by PCR (primers were 5'-CAA-TCTCCTCCTGTCCCTGTG-3' and 5'-ATCTCATCGCA-TCCCTGCGG-3') and subsequently subcloned in the pGEMT vector (Promega). Sense and antisense DIG-labelled riboprobes were synthesised by run-off transcription from SP6 and T7 promoters respectively (using a Boehringer kit). Whole mount RNA *in situ* hybridisations with *DmUpf1* sense and antisense probes were carried out essentially as described by Tautz and Pfeifle (30). After hybridisation and washes, anti-DIG-AP antibody (Boehringer, dilution 1:2000) was added for 2 h at room temperature. Following a series of washes in 1× PBT (1× PBS, 0.01% Triton X-100), alkaline phosphatase (AP) enzymatic reactions were carried out in AP buffer (100 mM NaCl, 50 mM MgCl<sub>2</sub>, 100 mM Tris-HCl pH 9.5, 0.01% Tween-20) with NBT/BCIP (Roche). Reactions were stopped by five rinses with 1× PBT. Embryos were dehydrated and rehydrated in a series of ethanol dilutions [30, 50, 70, 100% (v/v) and back] mounted in 80% glycerol and visualised under Nomarski optics in a Zeiss Axioplan microscope. Larval cuticles were mounted in Hoyer's:lactic acid (1:1), left to dry on a hot plate for ~24 h and observed using phase-contrast and dark-field microscopy. Digital photographs were taken with a Leica DFC 300 F camera and processed with Adobe Photoshop 5.0 software for Macintosh. Selection of *Ubx*<sup>195</sup> mutant embryos was performed through the use of GFP balancer chromosomes (see details above). Embryos were manually sorted according to their fluorescence level under a Leica MZ FLIII UV dissecting microscope and transferred to Eppendorf tubes. Parallel samples of wild type and mutant embryos were swiftly frozen in liquid N<sub>2</sub> and kept at -80°C until further processing.

### Real-time quantitative PCR

Total RNA was extracted from freshly collected, liquid N<sub>2</sub>-frozen embryo populations of selected ages using the RNeasy kit from Qiagen. RNAs were examined by gel, quantified by spectrophotometry, re-examined by gel and finally retro-transcribed using a SuperScript RT-PCR kit (Invitrogen) following manufacturer's instructions. Amplifications were performed with real-time TaqMan technology (PE Biosystems) and analysed using an ABI PRISM 7700 sequence detection system (Applied Biosystems). Thermocycler conditions were step 1: 50°C 2 min, step 2: 95°C 10 min, step 3: 95°C 15 s, step 4: 60°C 1 min, cycle back 45 times to step 3. The primers for *Ubx la* are as follows: forward 5'-CCGCCGTATTGTGTT-AAATCAG-3' (P2); reverse, 5'-GGCCAGCAATCACAC-ATTCTAC-3' (P1), and the TaqMan probe, 5'-CTTATC-

Upf1 protein family

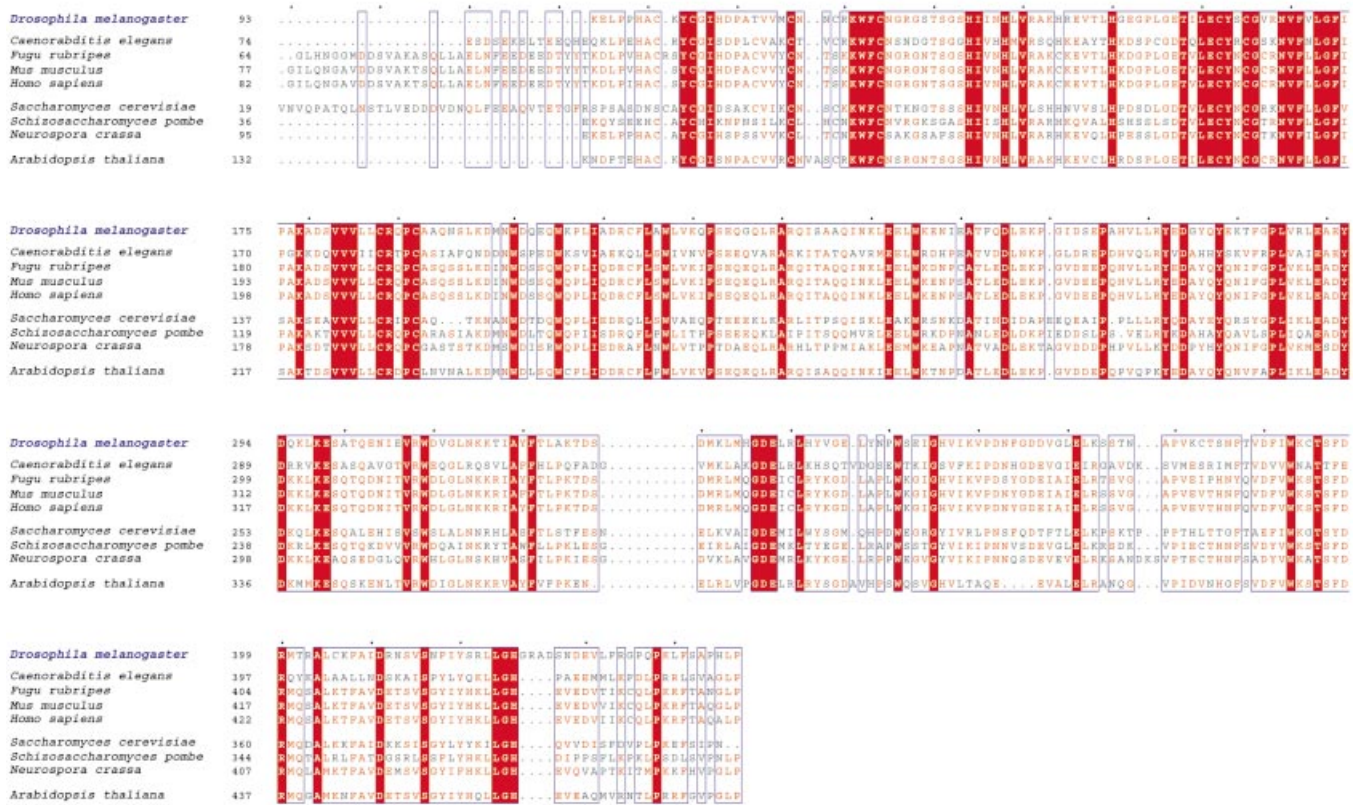


**Figure 1.** Sequence alignment of Upf1 proteins. Amino acid sequences corresponding to Upf1 proteins from different species. *Drosophila melanogaster* Upf1 (DmUpf1) shares extensive sequence homology with other members of the Upf1 protein family. Red letters indicate residues shared by many members of the family; red background indicates strict conservation of residues in all the species included in the study. Species names and SWISS PROT accession codes/ references for each sequence are as follows: *D.melanogaster* (SWP:Q9VYS3), *Caenorhabditis elegans* (SWP:O76512), *Fugu rubripes* (Q98TR3), *Mus musculus* (Q9EPU0), *Homo sapiens* (Q92900), *Saccharomyces cerevisiae* (NAM7/UPF1/MOF4), *Schizosaccharomyces pombe* (Q09820), *Neurospora crassa* (Q9HEH1) and *Arabidopsis thaliana* (Q9FJR0).

TTACCTGCGATAGCCATCCAGGG-3' (FAM labelled). The primers for *Ubx IVa* are as follows: forward 5'-TGTCGGCCGCGTCTTC-3' (P3); reverse, 5'-GGCCAGCAATCACACATTCTAC-3' (P1), and the TaqMan probe, 5'-CAGACCATTGTACCTGCGATAGCCATCC-3' (VIC labelled). Expression of the ribosomal protein 49 gene (*Rp49*) was used as an additional control for RNA loading and integrity. *Rp49* primers are forward 5'-GCGCACCAAGCACTTCATC-3'; reverse, 5'-GACGCACTCTGTTGTCGATACC-3' and *Rp49* TaqMan probe, 5'-ATATGCTAAGCTGTGCGACAAATGGC-3' (VIC labelled). Primer and probes were designed using Primer Express™ software (Applied Biosystems). TAMRA was used as the 3' quencher in all cases. After primer and probe optimisation experiments, all PCRs included 300 nM of each primer, 200 nM probe (*Ubx Ia*, *Ubx IVa* or *Rp49*) and 1× TaqMan® Universal PCR Master Mix (Applied Biosystems) containing the passive reference ROX. Experiments using different dilutions of plasmid templates for *Ubx Ia*, *Ubx IVa* and the mix (*Ubx Ia* + *Ubx IVa*) certified the specificity of the quantification procedure. The significance of differences in RNA abundance for different *Ubx* isoforms was assessed by evaluating threshold cycle ( $C_T$ ) values, according to the 'relative standard curve' method (ABI Prism 7700 Manual, available from

<http://www.appliedbiosystems.com>). For this, a sample obtained from a long collection of wild type embryos, showing high signals for both *Ubx* isoforms, was used as a calibrator. Reactions involving probes for *Ubx Ia* (FAM), *Ubx IVa* (VIC) and *Rp49* (VIC) were carried out in separate optical tubes fed from a series of reaction pre-mixes containing all PCR reagents (including time and genotype-specific templates) with the exception of probes and primers (which were supplied from gene-specific detection pre-mixes). Ratios of *Ubx Ia* and *Ubx IVa* abundances to *Rp49* were calculated to normalise signals. All real-time Taqman PCRs were done in triplicate. Whole experiments were repeated three times starting from new and independent embryo collections. Figures thus show each value as the mean ± SD of three independent experiments ( $n = 3$ ), with each one of them represented by the mean ± SD of three separate quantitative PCRs.

**RESULTS**

To explore the possibility that NMD affects developmental processes in *Drosophila*, we started by looking for the presence of conserved genetic components of the NMD machinery within the *Drosophila* genome. We focused our attention on the gene encoding Upf1, a protein that has been

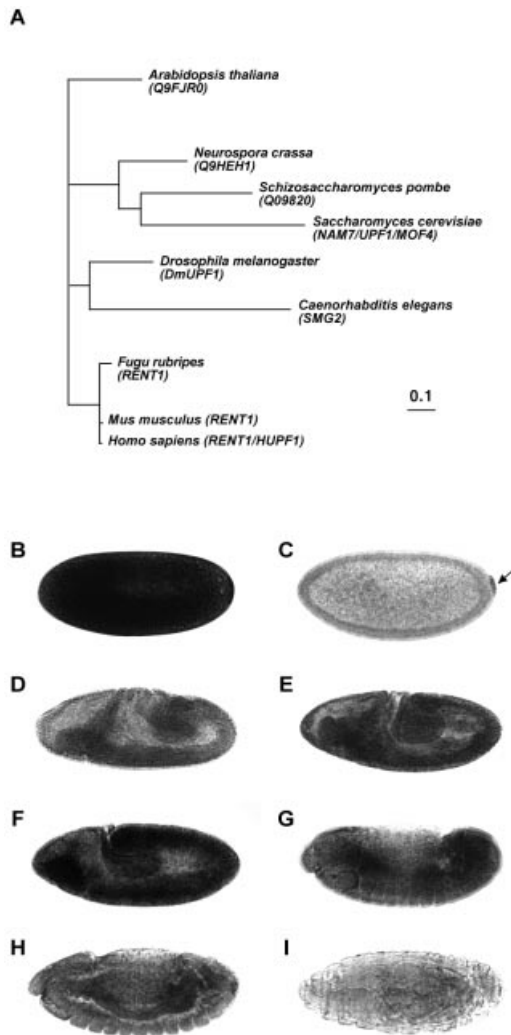


**Figure 2.** Phylogenetic and expression data on *DmUpf1*. (A) Phylogeny of the Upf1 protein family. Diagram showing a phylogenetic tree displaying the major relationships among sequences of the Upf1 protein family. Protein sequences are indicated by species name followed by gene name or accession code. (B–I) *DmUpf1* RNA expression at different developmental stages during *Drosophila* embryogenesis: (B) stage 2, (C) stage 5, (D) stage 7, (E) stage 8, (F) stage 9, (G) stage 12, (H) stage 14 and (I) stage 17. Note the high level of *DmUpf1* signal observed by stage 2, the localised signal detected at stage 5 (arrow) and the decrease of *DmUpf1* expression observed in late stages (G–I). Stages are according to Campos-Ortega and Hartenstein (41). In all panels, anterior is to the left and dorsal is up.

shown to be essential for an effective NMD response in all systems studied to date (25,26,31). Screening *Drosophila* genome databases (32) with the sequence of HUPF1 identifies one predicted gene, *CG1559*, encoding a protein with high amino acid similarity to HUPF1 (82%; Fig. 1). When *CG1559* is used as a probe within trans-specific databases it returns signals coding for Upf1 products from yeast, plant, worm, mouse and human. Sequence analysis of *CG1559*, here re-named *DmUpf1*, revealed that all the characteristic biochemical functions of Upf1 are accommodated within the predicted protein including putative zinc fingers in its N-terminal portion and all seven RNA helicase motifs that are present in Upf1 and other group I RNA helicases (33). Alignment of *DmUpf1* with other members of the Upf1

protein family reveals a high degree of amino acid conservation throughout the protein (Fig. 1). A phylogenetic analysis of the Upf1 protein family retrieves the major phylogenetic relationships among the groups included in the study, confirming the orthology of *DmUpf1*, and suggesting also that *Upf1* genes may be useful for phylogenetic purposes (Fig. 2A).

To study *DmUpf1* expression during *Drosophila* development we cloned a fragment of the *DmUpf1* gene by PCR and hybridised RNA probes prepared from this sequence to *Drosophila* embryos (see Materials and Methods). Consistent with data from other systems, we observe that *DmUpf1* is expressed in most tissues throughout development (Fig. 2B–I). Nonetheless, different expression phases can be distinguished. *DmUpf1* RNA is present at very high levels throughout early cleavage stage embryos, indicating a maternal contribution (Fig. 2B). The presence of this maternal product may reflect the necessity to have a fully operational RNA surveillance system while critical early embryonic genes are being expressed. At late blastoderm stages, levels of transcript decline, but localised *DmUpf1* RNA accumulation now becomes evident in the pole cells (Fig. 2C). After stage 5, *DmUpf1* RNA is expressed at varying levels in most or all tissues (Fig. 2D–F). Expression persists throughout much of embryogenesis, though in very late stages we note a decrease in the levels of *DmUpf1* RNA (Fig. 2G–I). Altogether, these sequence and expression data suggest that essential components of the NMD machinery are present during *Drosophila* embryonic development.

To test if NMD is actually operational during *Drosophila* development, we employed a nonsense mutation that affects the *Hox* gene *Ultrabithorax* (*Ubx*) (28). *Ubx* is expressed in a specific region along the antero–posterior axis of the animal body where it determines many aspects of segment morphology. This region, defined as parasegments 5 and 6, extends from the posterior compartment of the second thoracic segment to the anterior compartment of the first abdominal segment (29).

As a result of alternative splicing, the *Ubx* gene produces a family of closely related proteins or isoforms. *Ubx* isoforms differ from one another by the presence or absence of optional exons that separate the 5' exon from the 3' exon, which encodes the *Ubx* homeodomain (34,35). The *Ubx* nonsense allele that we used, *Ubx*<sup>195</sup>, carries a point mutation in the differentially spliced exon M2 (Fig. 3C) (36). This exon is only present in the longer versions of the protein, isoforms I and II (types a and b), and is spliced out from the short isoform IV (34,35) (Fig. 3C). *Ubx*<sup>195</sup> homozygotes die as larvae with defects in the CNS and tracheal system characteristic of a homeotic transformation of parasegments 5 and 6 to parasegment 4. Externally this transformation resembles that of a *Ubx* null mutant (Fig. 3A and B), but in the CNS *Ubx*<sup>195</sup> clearly retains some function, presumably mediated by *Ubx* isoform IV (36).

The location of the stop codon in *Ubx*<sup>195</sup> mutants establishes an experimental system that provides the exceptional opportunity of generating two qualitatively different types of mature mRNAs from the same promoter: PTC-bearing and PTC-exempt (Fig. 3C). If NMD is operational during *Drosophila* development, the abundance of messages for *Ubx* isoform Ia, including the premature stop codon, should be lower in *Ubx*<sup>195</sup>

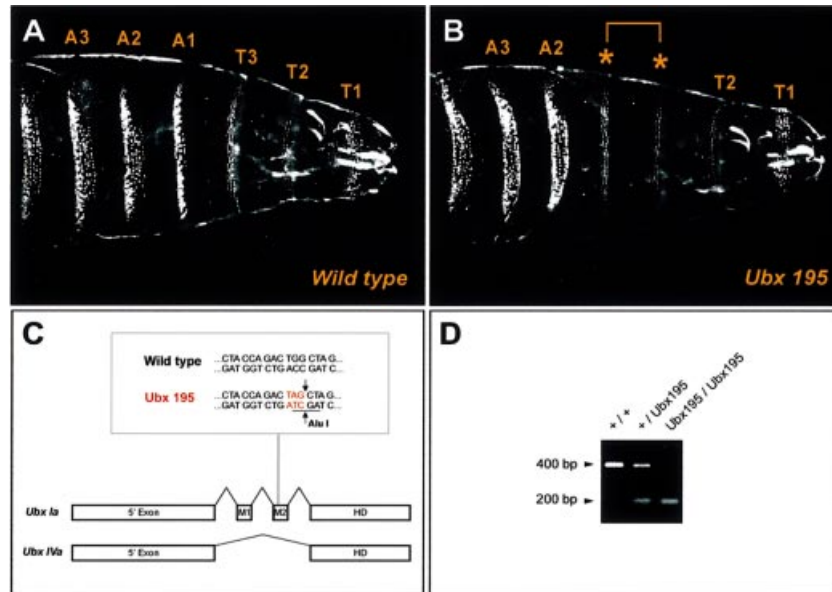


**Figure 3.** Phenotype of *Ubx<sup>195</sup>* mutants and structure of *Ubx* splicing isoforms investigated in this study. (**A** and **B**) Ventral cuticle phenotypes of wild type (**A**) and *Ubx<sup>195</sup>* (**B**) larvae. In *Ubx<sup>195</sup>* mutants, denticle belts of the third thoracic segment (T3, in parasegment 5) and the first abdominal segment (A1, in parasegment 6) are transformed to resemble that of T2 (parasegment 4) (asterisks). (**C**) Scheme of *Ubx* protein isoforms including (*Ubx Ia*) or excluding exon M2 (*Ubx IVa*). In *Ubx<sup>195</sup>* mutants, a G to A base substitution generates a PTC (red); this change also creates an *AluI* restriction site absent from the wild type sequence (underlined sequence). For simplicity, other *Ubx* isoforms that are not part of this study, such as *Ubx II* and all isoforms b, have been excluded from the diagram. (**D**) Presence of a restriction site for *AluI* within a 400 bp genomic PCR product including the exon M2, results in two small products of 200 bp that indicate the purity of the mutant embryo populations used in our study.

mutant embryos than in wild type embryos. On the other hand, the abundance of messages encoding *Ubx* isoform IVa, without the premature stop codon, should in principle be similar in both *Ubx<sup>195</sup>* and wild type embryos (see below). To test these predictions, we developed a real-time quantitative RT-PCR assay that allowed us to determine relative RNA levels coding for two *Ubx* isoforms: *Ubx Ia* and *Ubx IVa*. TaqMan fluorogenic probes were designed to match isoform-specific exon-exon junctions, thus avoiding amplification from genomic DNA (Fig. 4A) (see also Materials and Methods). *Ubx<sup>195</sup>* mutant chromosomes were maintained over a GFP-balancer, allowing the isolation of a homogeneous *Ubx<sup>195</sup>/Ubx<sup>195</sup>* embryo population (Fig. 3D) (see also Materials and Methods). Wild type and *Ubx<sup>195</sup>* embryos were collected for ~1 h and allowed to develop at 25°C. Total RNA was prepared from embryos of selected ages, quantified, retro-transcribed and used as template for real-time PCRs. An additional TaqMan probe was designed to detect the abundance of mRNA encoding *Rp49*, which served as an external control for RNA loading and integrity.

Results of *Ubx* and *Rp49* RNA quantification for wild type and *Ubx<sup>195</sup>* late embryos are shown in Figure 4B. All panels display amplification plots showing values of normalised fluorescence intensity ( $\Delta R_n$ ) versus amplification cycle, for both, wild type and *Ubx<sup>195</sup>* embryos (all assays in triplicate – see Materials and Methods). All samples show the same Ct for the control probe *Rp49*, thus certifying equal RNA loading in all cases. For *Ubx Ia*, Ct values for wild type samples are lower than those for *Ubx<sup>195</sup>* samples, indicating that levels for *Ubx Ia* are higher in wild type than in *Ubx<sup>195</sup>* embryos of similar age. This finding is consistent with a *Drosophila* NMD pathway operating on RNA messages containing PTCs. To test whether

PTC-free RNA isoforms derived from the *Ubx* transcription unit were or were not affected by NMD, we looked at the levels of *Ubx IVa* in the same RNA samples. Contrary to our expectations, we detected an increase in the levels of *Ubx IVa* message when comparing *Ubx<sup>195</sup>* embryos with wild types. This result suggests that the presence of a nonsense mutation could alter the balance between splicing isoforms of *Ubx*.

RNA levels coding for different *Ubx* isoforms fluctuate during embryonic development (34,35) so any discrepancy in the age distributions of embryos in wild type and *Ubx<sup>195</sup>* samples might cause an alteration in the ratio of isoforms. To control for this, we extracted RNA from a series of closely timed samples, choosing points in development when *Ubx* isoforms display major differences in tissue distribution (Fig. 5A). The outcome of these experiments is summarised in Figure 5 (B and C). *Ubx Ia* levels appear to be reduced in *Ubx<sup>195</sup>* embryos during most of embryogenesis (Fig. 5B). At the same time, levels of *Ubx IVa* RNA appear to be increased in *Ubx<sup>195</sup>* embryos (Fig. 5C). There is also some suggestion from our data that the magnitude of both these effects may vary during development.

## DISCUSSION

The widespread expression of *DmUpf1* throughout embryogenesis, and the effects of the *Ubx<sup>195</sup>* mutation on *Ubx Ia* transcript levels, suggest that NMD operates during *Drosophila* development. Our identification of *DmUpf1* together with a recent report identifying the *Drosophila* orthologues of the nematode *Smg5* and *Smg7* genes (37) provide the first information on the insect NMD genetic machinery.

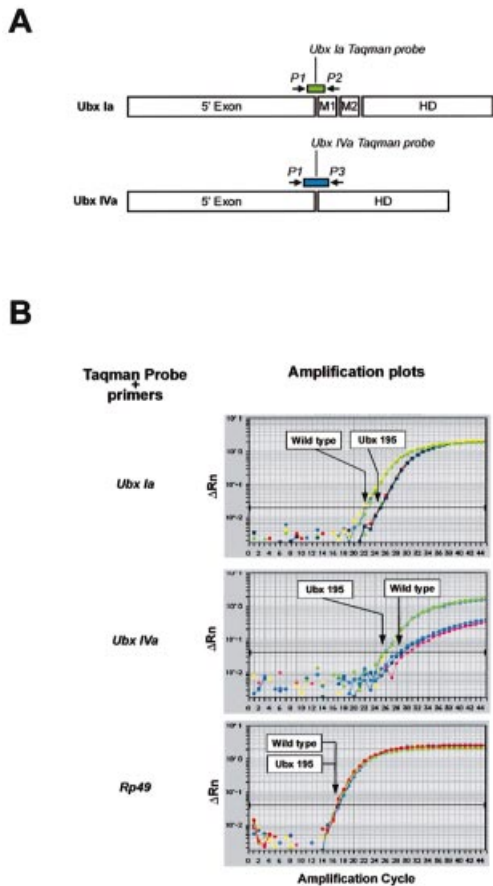


**Figure 4.** Quantification of *Ubx* isoforms in wild type and *Ubx<sup>195</sup>* embryos. (A) The location of primers (arrows) and Taqman probes (rectangles) is indicated. Please note that Taqman probes only hybridise to isoform-specific exon-exon junctions. This experimental design also prevents the detection of non-specific signals from traces of genomic DNA present in RNA preparations. (B) Amplification plots of real-time PCRs using *Ubx Ia*, *Ubx IVa* and Rp49 probes on wild type and *Ubx<sup>195</sup>* templates (late embryos). The plots relate PCR cycle number to changes ( $\Delta$ ) in detected fluorescence with background removed (Rn) on a logarithmic scale. Arrows highlight threshold cycle values (Ct) obtained for each genotype in the different reactions. The lower the Ct values, the higher the abundance of the RNA species detected by the system.

It would be desirable to test the developmental requirement for *DmUpf1* by eliminating its function. Unfortunately no candidate point mutations exist, and the available deficiencies covering the gene eliminate multiple gene functions, and severely disrupt embryonic development (data not shown). RNA interference (RNAi), in principle, provides an alternative way to knockout gene function, but in *Caenorhabditis elegans*, efficient operation of RNAi requires expression of *Upf1* (38), making this approach somewhat problematical. These considerations become even more complex in the context of a maternal contribution for *DmUpf1* as suggested by our expression data. Therefore, at present we do not know the null phenotype of *DmUpf1*.

The observed over-production of *Ubx IVa* in *Ubx<sup>195</sup>* embryos implies that the presence of a nonsense mutation in the *Ubx Ia* transcript, is able to affect the probability that it will be re-spliced to generate other isoforms. Effects of nonsense codons on alternative splicing have been

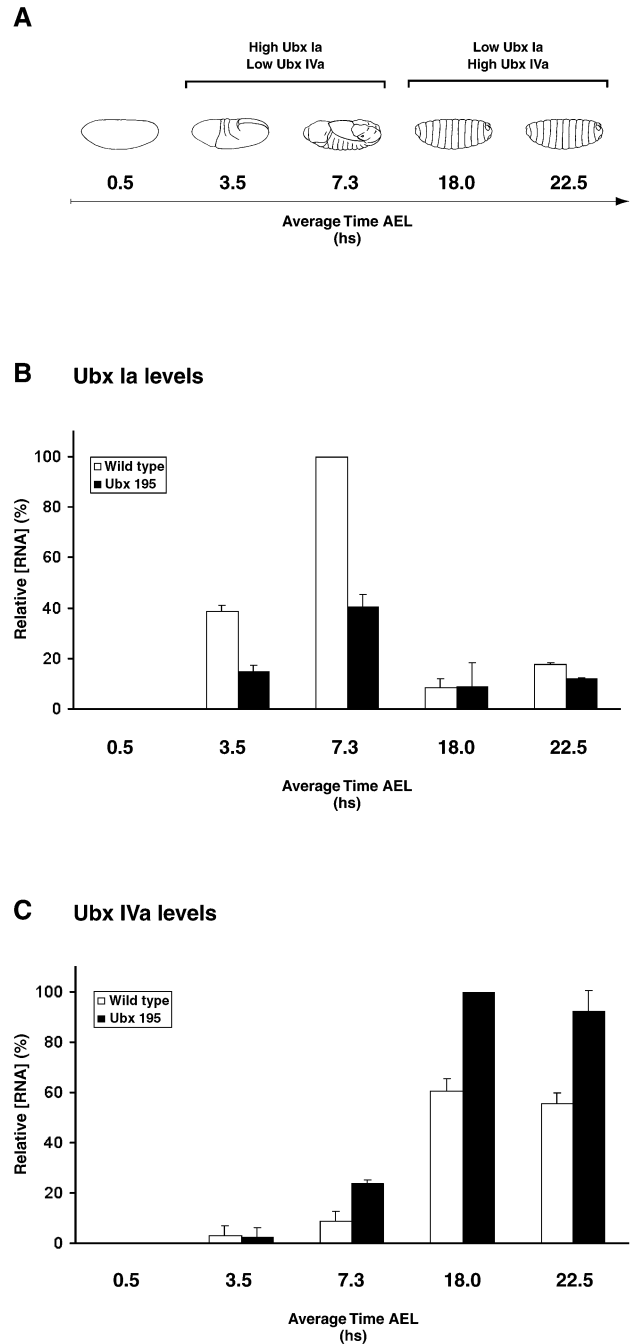


**Figure 5.** Expression profile of *Ubx* isoforms in wild type and *Ubx<sup>195</sup>* mutant embryos. (A) Diagram of embryos at various points in development (hours) as those analysed in RNA quantification experiments (AEL: after egg laying). Note that in wild type embryos, the highest expression levels for isoforms *Ubx Ia* and *Ubx IVa* are detected at different stages of embryogenesis. See also references (34,35). (B and C) Real-time quantitative PCR estimates of relative RNA levels for *Ubx Ia* (B) and *Ubx IVa* (C) in embryos at developmental times as shown in (A). White and black columns represent wild type and *Ubx<sup>195</sup>* samples, respectively. Sample groups displaying the highest RNA levels of their experimental series were arbitrarily assigned the value of 100%. For further details on real-time quantitative PCR, please refer to Materials and Methods.

documented in other systems (1,16) but, to our knowledge, never shown to affect developmental genes or processes. As mentioned in the introduction, NAS has initially been

explained as the consequence of the physical disruption of exonic splicing enhancers (ESEs) or silencers (ESSs) by nonsense mutations [reviewed in (16)]. However, very recent work shows that NAS could also result from reading frame disruptions (21,23,39). In spite of these stimulating advances, the molecular mechanisms behind NAS are still largely unclear.

It has been shown that *Ubx* isoform IVa is not produced by an exon-skipping mechanism, but instead through a complex re-splicing cycle from a *Ubx Ia* precursor transcript (40). In our system, *Ubx*<sup>195</sup> embryos produce less isoform Ia and more isoform IVa than their wild type counterparts, suggesting that NMD is not reducing the splicing precursor pool of *Ubx Ia* available for re-splicing, and may in fact be increasing the probability of such a re-splicing event.

As judged by the effects on the *Ubx* system, the efficiency of NMD does not seem to be constant throughout development (Fig. 5). Maximum NMD efficiency (as fold difference in *Ubx Ia* transcript levels between wild type and nonsense mutants) occurs between ~3 and 8 h after egg laying (Fig. 5 and data not shown). The magnitude of these effects is in line with previous reports on NMD activity in other systems. Interestingly, this also coincides with the times at which *DmUpf1* is expressed at high levels in most embryonic tissues. The efficiency of NMD seems to decrease at a time when *DmUpf1* signal falls (Figs 2 and 5). Perhaps the availability of different amounts of *DmUpf1* accounts for the variable efficiency of NMD. However, here we must be cautious in assuming a causal relationship, since *DmUpf1* is only one component of the NMD machinery and we only observed its RNA levels. Another possibility is that developmental oscillations in the transcriptional levels of nonsense-RNA templates susceptible to NMD could lead to variability in the nonsense-RNA fraction escaping NMD control.

Perhaps a limitation of our *Ubx* system in live embryos is that it does not allow us to estimate the individual contributions of NMD and NAS activities to the net *Ubx* RNA levels. Future studies involving nonsense and wild type *Ubx* splicing mini-genes, expressed in cell culture and transgenic animals, will help us to determine the extent of the developmental effects of NMD and NAS on isoform steady levels.

Biological processes as fundamental as sex determination have been shown to involve the generation of alternative transcripts containing PTCs, the usual assumption being that these messages would lead to the production of non-functional truncated proteins. Our findings, demonstrating that NMD is operational during *Drosophila* development, imply that other mechanisms may need to be considered.

## ACKNOWLEDGEMENTS

We wish to thank Philippa Smith and Andrew McKenzie for their assistance with real-time PCR, Javier Lopez for kindly providing fly stocks, Chuck Cook for help with phylogenetic analysis and Juliane Mossinger, Cassandra Extavour, Elio Sucena, Henrique Teotonio and Vitor Barbosa for general advice and encouragement. We also thank two anonymous referees for their constructive criticism. This work was supported by The Wellcome Trust.

## REFERENCES

- Hentze, M.W. and Kulozik, A.E. (1999) A perfect message: RNA surveillance and nonsense-mediated decay. *Cell*, **96**, 307–310.
- Maquat, L.E. and Li, X. (2001) Mammalian heat shock p70 and histone H4 transcripts, which derive from naturally intronless genes, are immune to nonsense-mediated decay. *RNA*, **7**, 445–456.
- LeHir, H., Izaurralde, E., Maquat, L.E. and Moore, M.J. (2000) The spliceosome deposits multiple proteins 20–24 nucleotides upstream of mRNA exon–exon junctions. *EMBO J.*, **19**, 6860–6869.
- LeHir, H., Moore, M.J. and Maquat, L.E. (2000) Pre-mRNA splicing alters mRNP composition: evidence for stable association of proteins at exon–exon junctions. *Genes Dev.*, **14**, 1098–1108.
- Zhou, Z., Luo, M.J., Straesser, K., Katahira, J., Hurt, E. and Reed, R. (2000) The protein Aly links pre-messenger-RNA splicing to nuclear export in metazoans. *Nature*, **407**, 401–405.
- Dreyfuss, G., Kim, V.N. and Kataoka, N. (2002) Messenger-RNA-binding proteins and the messages they carry. *Nature Rev. Mol. Cell Biol.*, **3**, 195–205.
- Cheng, J., Belgrader, P., Zhou, X. and Maquat, L.E. (1994) Introns are *cis* effectors of the nonsense-codon-mediated reduction in nuclear mRNA abundance. *Mol. Cell Biol.*, **14**, 6317–6325.
- Nagy, E. and Maquat, L.E. (1998) A rule for termination-codon position within intron-containing genes: when nonsense affects RNA abundance. *Trends Biochem. Sci.*, **23**, 198–199.
- Lykke-Andersen, J., Shu, M.D. and Steitz, J.A. (2001) Communication of the position of exon–exon junctions to the mRNA surveillance machinery by the protein RNPS1. *Science*, **293**, 1836–1839.
- Wilkinson, M.F. and Shyu, A.B. (2002) RNA surveillance by nuclear scanning? *Nature Cell Biol.*, **4**, E144–147.
- Gonzalez, C.I., Bhattacharya, A., Wang, W. and Peltz, S.W. (2001) Nonsense-mediated mRNA decay in *Saccharomyces cerevisiae*. *Gene*, **274**, 15–25.
- Czaplinski, K., Ruiz-Echevarria, M.J., Paushkin, S.V., Han, X., Weng, Y., Perlick, H.A., Dietz, H.C., Ter-Avanesyan, M.D. and Peltz, S.W. (1998) The surveillance complex interacts with the translation release factors to enhance termination and degrade aberrant mRNAs. *Genes Dev.*, **12**, 1665–1677.
- Lykke-Andersen, J. (2001) mRNA quality control: marking the message for life or death. *Curr. Biol.*, **11**, R88–91.
- Thermann, R., Neu-Yilik, G., Deters, A., Frede, U., Wehr, K., Hagemeyer, C., Hentze, M.W. and Kulozik, A.E. (1998) Binary specification of nonsense codons by splicing and cytoplasmic translation. *EMBO J.*, **17**, 3484–3494.
- Buhler, M., Wilkinson, M.F. and Muhlemann, O. (2002) Intranuclear degradation of nonsense codon-containing mRNA. *EMBO Rep.*, **3**, 646–651.
- Maquat, L.E. (2002) NASTy effects on fibrillin pre-mRNA splicing: another case of ESE does it, but proposals for translation-dependent splice site choice live on. *Genes Dev.*, **16**, 1743–1753.
- Brogna, S., Sato, T.A. and Rosbash, M. (2002) Ribosome components are associated with sites of transcription. *Mol. Cell*, **10**, 93–104.
- Iborra, F.J., Jackson, D.A. and Cook, P.R. (2001) Coupled transcription and translation within nuclei of mammalian cells. *Science*, **293**, 1139–1142.
- Valentine, C.R. (1998) The association of nonsense codons with exon skipping. *Mutat. Res.*, **411**, 87–117.
- Li, S., Leonard, D. and Wilkinson, M.F. (1997) T cell receptor (TCR) mini-gene mRNA expression regulated by nonsense codons: a nuclear-associated translation-like mechanism. *J. Exp. Med.*, **185**, 985–992.
- Wang, J., Hamilton, J.I., Carter, M.S., Li, S. and Wilkinson, M.F. (2002) Alternatively spliced TCR mRNA induced by disruption of reading frame. *Science*, **297**, 108–110.
- Mendell, J.T., ap Rhys, C.M. and Dietz, H.C. (2002) Separable roles for *rent1/hUpf1* in altered splicing and decay of nonsense transcripts. *Science*, **298**, 419–422.
- Wang, J., Chang, Y.F., Hamilton, J.I. and Wilkinson, M.F. (2002) Nonsense-associated altered splicing: a frame-dependent response distinct from nonsense-mediated decay. *Mol. Cell*, **10**, 951–957.
- Moore, M.J. (2002) RNA events. No end to nonsense. *Science*, **298**, 370–371.
- Leeds, P., Peltz, S.W., Jacobson, A. and Culbertson, M.R. (1991) The product of the yeast *UPF1* gene is required for rapid turnover of mRNAs

- containing a premature translational termination codon. *Genes Dev.*, **5**, 2303–2314.
26. Pulak,R. and Anderson,P. (1993) mRNA surveillance by the *Caenorhabditis elegans* smg genes. *Genes Dev.*, **7**, 1885–1897.
  27. Medghalchi,S.M., Frischmeyer,P.A., Mendell,J.T., Kelly,A.G., Lawler,A.M. and Dietz,H.C. (2001) Rent1, a trans-effector of nonsense-mediated mRNA decay, is essential for mammalian embryonic viability. *Hum. Mol. Genet.*, **10**, 99–105.
  28. Lewis,E.B. (1978) A gene complex controlling segmentation in *Drosophila*. *Nature*, **276**, 565–570.
  29. Morata,G. and Kerridge,S. (1981) Sequential functions of the bithorax complex of *Drosophila*. *Nature*, **290**, 778–781.
  30. Tautz,D. and Pfeifle,C. (1989) A non-radioactive in situ hybridization method for the localization of specific RNAs in *Drosophila* embryos reveals translational control of the segmentation gene hunchback. *Chromosoma*, **98**, 81–85.
  31. Sun,X., Perlick,H.A., Dietz,H.C. and Maquat,L.E. (1998) A mutated human homologue to yeast Upf1 protein has a dominant-negative effect on the decay of nonsense-containing mRNAs in mammalian cells. *Proc. Natl Acad. Sci. USA*, **95**, 10009–10014.
  32. Adams,M.D., Celniker,S.E., Holt,R.A., Evans,C.A., Gocayne,J.D., Amanatides,P.G., Scherer,S.E., Li,P.W., Hoskins,R.A., Galle,R.F. *et al.* (2000) The genome sequence of *Drosophila melanogaster*. *Science*, **287**, 2185–2195.
  33. Koonin,E.V. (1992) A new group of putative RNA helicases. *Trends Biochem. Sci.*, **17**, 495–497.
  34. Kornfeld,K., Saint,R.B., Beachy,P.A., Harte,P.J., Peattie,D.A. and Hogness,D.S. (1989) Structure and expression of a family of Ultrabithorax mRNAs generated by alternative splicing and polyadenylation in *Drosophila*. *Genes Dev.*, **3**, 243–258.
  35. O'Connor,M.B., Binari,R., Perkins,L.A. and Bender,W. (1988) Alternative RNA products from the Ultrabithorax domain of the bithorax complex. *EMBO J.*, **7**, 435–445.
  36. Weinzierl,R., Axton,J.M., Ghysen,A. and Akam,M. (1987) Ultrabithorax mutations in constant and variable regions of the protein coding sequence. *Genes Dev.*, **1**, 386–397.
  37. Chiu,S.Y., Serin,G., Ohara,O. and Maquat,L.E. (2003) Characterization of human Smg5/7a: a protein with similarities to *Caenorhabditis elegans* SMG5 and SMG7 that functions in the dephosphorylation of Upf1. *RNA*, **9**, 77–87.
  38. Domeier,M.E., Morse,D.P., Knight,S.W., Portereiko,M., Bass,B.L. and Mango,S.E. (2000) A link between RNA interference and nonsense-mediated decay in *Caenorhabditis elegans*. *Science*, **289**, 1928–1931.
  39. Li,B., Wachtel,C., Miriami,E., Yahalom,G., Friedlander,G., Sharon,G., Sperling,R. and Sperling,J. (2002) Stop codons affect 5' splice site selection by surveillance of splicing. *Proc. Natl Acad. Sci. USA*, **99**, 5277–5282.
  40. Hatton,A.R., Subramaniam,V. and Lopez,A.J. (1998) Generation of alternative Ultrabithorax isoforms and stepwise removal of a large intron by resplicing at exon–exon junctions. *Mol. Cell*, **2**, 787–796.
  41. Campos-Ortega,J.A. and Hartenstein,V. (1997) *The embryonic development of Drosophila melanogaster*. 2nd Edn. Springer Verlag, Berlin, Germany.